NIH Public Access
Author Manuscript
Anal Chem. Author manuscript; available in PMC 2010 October 7.

Published in final edited form as:
Anal Chem. 2009 October 1; 81(19): 8048–8053. doi:10.1021/ac901479e.

Ultrafast Differential Ion Mobility Spectrometry at Extreme Electric Fields Coupled to Mass Spectrometry

Alexandre A. Shvartsburg[*], **Keqi Tang**[*], **Richard D. Smith**[*], **Martin Holden**[†], **Martyn Rush**[†], **Andrew Thompson**[†], and **Danielle Toutoungi**[†]

[*]Biological Sciences Division, Pacific Northwest National Laboratory, P.O. Box 999, Richland, WA 99352

[†]Owlstone Ltd, 127 Cambridge Science Park, Cambridge, CB4 0GD, United Kingdom

Abstract

Microchip-based field asymmetric waveform ion mobility spectrometry (FAIMS) analyzers featuring a grid of 35 μm - wide channels have allowed electric field intensity (*E*) over 60 kV/cm, or about twice that in previous devices with >0.5 mm gaps. Since the separation speed scales as E^4 to E^6, these chips filter ions in just ~20 μs (or ~100 – 10,000 times faster than "macroscopic" designs), although with reduced resolution. Here we report integration of these chips into electrospray ionization (ESI) mass spectrometry, with ESI coupled to FAIMS via a curtain plate/orifice interface with edgewise ion injection into the gap. Adjusting gas flows in the system permits control of ion residence time in FAIMS, which affects resolving power independently of ion desolvation after the ESI source. The results agree with *a priori* simulations and scaling rules. Applications illustrated include analyses of amino acids and peptides. Because of limited resolving power, the present FAIMS units are suitable to distinguish compound classes more than individual species. In particular, peptides separate from many other classes, including PEGs that are commonly encountered in proteomic analyses. In practical analyses with realistic time constraints, the effective separation power of present FAIMS may approach that of "macroscopic" systems.

Introduction

For analyses of complex biological or environmental samples, mass spectrometry (MS) is increasingly combined with ion mobility spectrometry (IMS) that distinguishes ion species based on transport properties in a non-reactive buffer gas.[4–13] Several IMS/MS platforms have been commercialized in the last few years, and more MS instruments allow an IMS option. Some systems, such as HDMS Synapt (Waters),[12,13] employ conventional IMS meaning that ions are sorted by absolute mobility, *K*. However, the mobilities for ions in gases depend on the ratio of electric field intensity (*E*) to the gas number density (*N*), and the relative deviation (α) from the zero-field mobility *K*(0) can be expanded in infinite series of even powers[1,3] over *E*/*N*:

$$K(E/N)=K(0)[1+\alpha(E/N)]=K(0)[1+a_1(E/N)^2+a_2(E/N)^4+\ldots+a_n(E/N)^{2n}] \quad (1)$$

This effect is exploited in differential IMS or FAIMS to filter ions by the difference between *K* at two *E*/*N* magnitudes.[3] This is achieved using a periodic time-dependent electric field *E*(*t*) with alternating segments of high *E* and lower *E* of opposite polarity but null mean *E*, in which ions drift with velocity proportional to the difference between the α values in these segments. The field is established in a gap between two electrodes through which ions are pulled by gas flow.[3] For any given species, the drift across the gap (that would result in ions neutralized on an electrode) can be offset by motion induced by constant "compensation

NIH-PA Author Manuscript
NIH-PA Author Manuscript
NIH-PA Author Manuscript

NIH-PA Author Manuscript

NIH-PA Author Manuscript

NIH-PA Author Manuscript

field" (E_C) added to $E(t)$; scanning E_C produces the FAIMS spectrum.[3] The E_C values depend on the $E(t)$ amplitude (the "dispersion field", E_D), and analytes are better characterized by maps[3] of E_C versus E_D. The species with equilibrium E_C close to the actual value may still pass the gap because of its finite width, diffusion, and ion-ion interactions, which jointly control the resolution of FAIMS.[3]

As the values of a function and its derivative are, in principle, independent, FAIMS and conventional IMS separations can be largely orthogonal.[7] This is not the case for conventional IMS and MS, as mobility is proportional to the inverse ion-molecule collision cross section and thus tightly correlated to the ion size and mass. The derivative of $K(E/N)$ is not as closely related to the ion mass, and FAIMS and MS dimensions are less correlated and may be near-orthogonal. [3,7] This advantage has stimulated rapid development of the FAIMS/MS technology and its adoption in the quadrupole, ion trap, and orbitrap MS products by Thermo Fisher.[14]

The FAIMS electrodes may be curved (for example, cylindrical or spherical), creating an inhomogeneous electric field that focuses ions, or planar with a homogeneous field and thus no focusing.[3,5,14–16] In the result, a planar FAIMS has advantages over the curved form in terms of resolution and the inherent resolution/sensitivity balance, quantification accuracy, and duty cycle for broad analyses,[16] and current FAIMS[17,18] and GC/FAIMS[19,20] instruments use planar FAIMS designs. However, commercial FAIMS/MS systems have employed cylindrical FAIMS, where the focusing and geometry allow the ion beam to be constrained and effectively extracted through a small circular orifice.[5] This permits ready coupling to MS, while diffuse ion beams in previous planar FAIMS systems could not be transmitted through standard MS inlets without huge losses. The slit-aperture inlets provide major improvement, but losses remain.[16,21,22]

FAIMS analyses using "macroscopic" devices with a gap width (g) of 0.5 – 2.5 mm (for any geometry) had required a minimum ion residence time of t ~1 – 200 ms at a given E_C and thus ~0.1 – 30 s for a full E_C scan. This has limited the utility of inserting FAIMS between liquid-phase separations such as liquid chromatography (LC) or capillary electrophoresis (CE) and MS, where several FAIMS scans should generally be acquired during the elution of a single LC or CE feature. To accomplish that in conjunction with regular LC,[23,24] scanning E_C was replaced by stepping in large increments, which has compressed the FAIMS cycle but dropped the resolution below that obtainable, thus reducing the gain from FAIMS filtering. The best FAIMS specificity is provided by $\{E_C; E_D\}$ maps, but those take at least an order of magnitude longer time to collect than a single E_C scan and thus were incompatible with online LC/MS analyses.

In general, the E_D value in FAIMS is capped by the lower of (i) the onset of the destruction of ions due to field heating,[25–27] (ii) hardware constraints on the voltage that creates the waveform, and (iii) the threshold for electrical breakdown of the gas. While the limit (i) is fundamental, (ii) and (iii) are engineering factors. According to the Paschen law,[28] (iii) depends on the gas pressure and gap width and can be lifted by reducing either, though narrowing the gap is more effective.[27] The recently developed FAIMS microchips[27] with g = 35 μm permit E_D to be raised from ~20 – 30 kV/cm in previous macro units to >60 kV/cm. Since the separation speed scales as the *fourth to sixth* power of E_D, this increase would accelerate the separation at equal resolving power (R) by over an order of magnitude.[27] Present chips have lower R than previous FAIMS devices, but filter ions in just ~20 μs, or ~10^2 – 10^4 times faster. For effective transmission of high ion currents, the chips feature multiple parallel gaps. The performance of stand-alone FAIMS analyzers based on these chips has been evaluated for small ions generated by β-radiation sources and found in agreement with first-principles calculations.[27]

NIH-PA Author Manuscript

NIH-PA Author Manuscript

NIH-PA Author Manuscript

Here, we report the integration of multichannel FAIMS chips using extreme fields with MS and ESI sources, which extends exceptionally fast FAIMS/MS analyses to a broad range of complex samples, including biological ions.

Experimental Methods

The ESI process generates clustered ions that must be desolvated prior to FAIMS, for example using a gas counter flow in a curtain plate/orifice interface.[5,14,16,29] Here, such an interface is built in front of the PEEK plate holding the FAIMS chip. The circular apertures in the curtain and orifice plates have diameters of 3.2 and 2.0 mm, respectively. Those values keep close to the ratio of 5:3 used in previous ESI/FAIMS interfaces,[16] but are larger by ~30% to maximize ion transmission into the chip that has a large acceptance area (3.25 × 2.5 mm).[27] The ESI source is an emitter positioned a few mm away from the curtain plate aperture, with the distance and angle adjusted to optimize the ion signal. The (N_2) carrier gas flows to the interface at Q_{in} = 0 – 3.2 L/min and is partitioned into two streams, one leaving through the aperture in the curtain plate and the other carrying ions via the aperture in the orifice plate into the chip (Fig. 1). Unlike previous designs where the curtain and orifice plates were parallel to the FAIMS gap and desolvated ions entered the gap through one of the electrodes,[5,14,16,29] here the plates are perpendicular to the gap and ions enter it edgewise. This allows in-line processing of ion beams without bending, which should reduce losses in the ESI/FAIMS interface.

All ESI/MS interfaces employ the above curtain plate/orifice concept or a capillary where traversing ions are thermally desolvated. As with other FAIMS analyzers to date, the present chip is coupled to a commercial MS platform with capillary inlet, here the LTQ ion trap (Thermo Fisher). Since ions exiting FAIMS were already desolvated in the ESI/FAIMS interface and/or upon injection into FAIMS by field heating,[25,26] the capillary is held at 70 °C. The plate holding the chip is housed in a vacuum-tight chamber sealed to the inlet, with an air gap to the capillary of 1.1 mm. The chamber is evacuated by a rotary vane pump (Rietschle Thomas G045) at a flow of Q_{out} = 0 – 3.2 L/min, measured to ~1.5 % error by a mass flow controller. The flow through the capillary (i.d. = 0.5 mm) is Q_{ms} ~0.8 L/min, hence the flow through the chip is (Fig. 1)

$$Q = Q_{out} + Q_{ms} \tag{2}$$

which ranges from ~0.8 to ~4 L/min, and the outflow through curtain plate is

$$Q_{cu} = Q_{in} - Q = Q_{in} - Q_{out} - Q_{ms} \tag{3}$$

The mean ion residence time in a gap of volume V equals[30]

$$t \sim 0.7\, V/Q \tag{4}$$

The coefficient 0.7 reflects that the ions selected by FAIMS have mainly passed near the gap median, where the flow is faster than the average over the gap.[30] With V = 1.2 mm^3 for these chips, t ranges from ~63 to ~13 μs. Hence all flows in the system and the FAIMS separation time and extent of ion desolvation in front can be independently controlled by varying Q_{in} and Q_{out}.

In operation, the MS inlet is grounded. For cations, the other voltages (relative to ground) are 30 V on the chip, 50 V on the orifice plate, and 0 – 2 kV on the curtain plate. The ESI emitter is biased at ~1 – 3 kV above the curtain plate. For anions, the values become negative. The

NIH-PA Author Manuscript

NIH-PA Author Manuscript

NIH-PA Author Manuscript

sample is infused to the emitter by a syringe pump at a flow rate of 0.5 μL/min. The ion trap was scanned in MS mode over the *m*/*z* range of 150 – 2000 in ~110 ms, using the AGC target value of 3×10^4 and maximum ion injection time of 10 ms. The size of the chip housing in the FAIMS/MS configuration has required lengthening the electric leads of waveform power supply compared to the stand-alone FAIMS,[27] which has increased the circuit capacitance and thus lowered the waveform frequency from 28.5 to 22.2 MHz.

The charge detector after the chip is not biased so as to pass most ions to MS, but some ions still reach it and one can monitor the FAIMS spectra while acquiring the FAIMS/MS data.[27] The ion losses due to the FAIMS stage were measured by comparing the ion counts for same analytes in the ESI/MS and ESI/FAIMS/MS configurations. As expected,[27] the transmission increases for larger ions with lower mobility and diffusion coefficients, but is ~10 – 20% for medium-size species relevant to biological analyses as exemplified below. These values are less than those calculated for the chip proper,[27] suggesting significant losses in the FAIMS interfaces. Optimization of those interfaces to improve the ion utilization is in progress.

The system was evaluated in the cation mode using the ~1 μM solutions of reserpine (a prevalent MS standard), amino acid leucine, or a mixture of 4 peptides [bradykinin (1060 Da), angiotensin I (1296 Da), fibrinopeptide a (1536 Da), and neurotensin (1672 Da)] in 50:49:1 water/methanol/acetic acid. In some experiments, to emulate a realistic matrix, lab wastewater containing complex proteome digests, other accidental pollutants, and (optionally) a customary MS calibrant polyethelene glycol (PEG) was added to the sample.

Results

Demonstration of FAIMS/MS analyses

The operation of the FAIMS stage in the ESI/FAIMS/MS system was optimized using reserpine solutions, with protonated reserpine (*m*/*z* = 609) dominating the ion flux (Fig. 2a). The signal for this species improved with increasing curtain plate voltage U_C until the saturation at ~1.2 kV (Fig. 2b), and we adopted that value.

The peaks for (H^+)reserpine move to higher E_C/N at greater E_D, reaching 1.1 Td at the maximum E_D/N = 250 Td (Fig. 2c). With $E_D > 0$, a positive E_C that rises at higher E_D means a mobility decreasing with increasing field. This classifies the ion as “type C” in line with previous data at absolute E_D/N < ~80 Td, where $|E_C / N|$ was under 0.06 Td.[16,22] (Those data were for $E_D < 0$, hence $E_C < 0$). The E_C value scales as E_D^3 (Fig. 2d), as expected when the terms with $n > 1$ in eq (1) are negligible relative to the $n = 1$ term.[3] Appropriately for planar gaps,[3,31,32] the peak width (*w* for fwhm) is independent of E_D within 5% (Fig. 2c). As reducing suction after the chip extends the separation time, the peak narrows from w = 0.8 Td at Q_{out} = 2.5 L/min (where t ~15 μs) to 0.5 Td at Q_{out} = 0.7 L/min and t ~34 μs (Fig. 2e). This trend matches the simulations assuming the measured[33] K_0 = 0.73 $cm^2/(Vs)$ and is close to the predicted[31] scaling of resolving power of planar FAIMS as $t^{1/2}$ (Fig. 2f). These results evidence that FAIMS microchips can be coupled to mass spectrometry effectively and that existing models adequately describe the separations in that arrangement.

To illustrate separation of different species and chemical noise removal in realistic samples, we analyzed a solution of leucine (Leu) with added wastewater. Positive-mode ESI frequently produces protonated monomers and proton-bound dimers (and possibly larger oligomers) for many small and medium-size species, including amino acids and peptides. With moderately concentrated Leu solutions, H^+Leu (*m*/*z* = 132) and $H^+(Leu)_2$ (*m*/*z* = 263) are normally observed. Here those features are seen on a dense background of intense peaks extending from *m*/*z* = 146 to the upper limit of analysis at *m*/*z* = 1300 (Fig. 3a). The FAIMS spectra obtained at and near the maximum E_D/N exhibit two peaks (Fig. 3b) - one (at lower E_C/N) heavily

NIH-PA Author Manuscript

NIH-PA Author Manuscript

NIH-PA Author Manuscript

enriched in H^+Leu and the other comprising $H^+(Leu)_2$ and almost all other ions (Fig. 3c). Thus FAIMS filtering raises the s/n ratio for H^+Leu (with noise summed over the full *m*/*z* range) by ~20 times.

In previous FAIMS analyses[16,34,35] at E_D/N < ~80 Td, the H^+Leu displayed "type A" behavior where mobility rises in stronger fields, leading to E_C < 0 that decreases at higher E_D. Here, at E_D/N = 225 – 250 Td, we find E_C = (0.1 – 0.4) Td > 0 that increases at higher E_D (Fig. 3b), indicating a type C species. This transition is similar to that observed for DMMP cations and DNT anions in stand-alone FAIMS,[27] but here both coefficients a_1 and a_2 fit to the data at E_D/N < 80 Td are positive[35] and hence the decrease of K at higher E_D/N must be due to negative a_n for n = 3 or greater. Such conversion to type C at sufficiently high $|E_D / N|$ is universal for type A ions: with increasing energy, the ion-molecule collisions always transition from sampling the potential well to hard scattering on the repulsive wall that is manifested as the type C behavior.[3,36]

Peptide separations

The introduction of FAIMS into the LC/ESI/MS pipeline has largely been motivated by the need for high-throughput analyses of complex peptide mixtures and low-level detection of target components,[23] and bottom-up proteomics is a topical area of FAIMS application.[11,23,24] Tryptic peptide ions generated by ESI have typical charge states (*z*) of 1 – 4. In the previous FAIMS studies using N_2 at $|E_D / N|$ ~80 Td, those ions behaved as type C with $|E_C / N|$ in the ~0.04 – 0.4 Td range.[24,37–40] As $|E_C|$ values generally increased for higher *z*, FAIMS has roughly fractionated electrosprayed digests[7,23,24,37,38] by *z*, in particular separating 1+ species from higher *z*. Peptides of equal *z* usually had closer $|E_C|$ and thus were harder to distinguish than those with different *z*.

Here we analyzed the peptide mixture in clean solution or a matrix containing wastewater and PEGs. All four peptides remain type C ions with E_C/N of ~1.6 – 2.5 Td (at E_D/N = 250 Td), Fig. 4a. This enables fairly clean filtering of peptide ions from other species that all have E_C/N < ~1.3 Td, including those with similar *m*/*z* such as several series of peaks spaced by *m*/*z* = 44 that are presumed PEG derivatives (Fig. 4 b – d). Although those species are singly-charged, all three peptides detected with *z* = 1 pass FAIMS within the peptide feature (albeit at its low-E_C side) and not the contaminant peak (Fig. 4a). By varying the gas flow, we could adjust the resolution to pass all peptides at once (at E_C/N ~2 Td), but almost no other ions. Peptides as a class could not be selected using "macro-FAIMS", where the resolution is too high to pass all or most peptides together.

The present chip can generally separate peptide ions of same or different charge states from each other only in part even at the maximum E_D/N, because of low instrumental resolving power but also conformational diversity. For example, at the shortest residence time in FAIMS (Fig. 5a), the features for bradykinin 2+ (B2) and neurotensin 2+ (N2) have respective *w* of 0.8 and 0.9 Td that exceed the calculated widths of 0.60 and 0.56 Td [using the K_0 measured[41,42] at room temperature: 1.22 cm^2/(Vs) for B2 and 0.96 cm^2/(Vs) for N2]. As the modeled widths for the DMMP[27] and reserpine (Fig. 2f) ions match the experiment, this discrepancy suggests (more so for B2) the presence of multiple peptide folds that are ubiquitous for protein ions in FAIMS[16] and DT IMS[43,44] studies and have been found for B2 and N2 in high-resolution FAIMS.[16,22] Even then, the ~0.6 Td spacing between the apexes of N2 and B2 features (corresponding to the major conformers) suffices only for their separation at about half-height (Fig. 5a). Extending *t* to ~39 μs via slowing the flow to a practical minimum reduces the computed widths to ~0.35 – 0.38 Td (Fig. 5b). The measured N2 peak narrows by a similar ~0.2 Td, and a lesser narrowing and pronounced shoulder on the low-E_C side of B2 feature indicate abundant minor conformer(s), as observed previously.[16,22,40] The tailing toward higher E_C for both peaks seems due to ion-molecule clustering that results from penetration of

NIH-PA Author Manuscript

NIH-PA Author Manuscript

NIH-PA Author Manuscript

ESI solvent vapors into FAIMS, and can be suppressed with better desolvation. Importantly, the major conformers of N2 and B2 are now separated near the baseline (Fig. 5b). The intensity of B2 relative to N2 drops in longer analyses because B2 ions have higher mobility and thus are eliminated from the gap by diffusion faster.

At $|E_D/N|$ ~ 80 Td, the $|E_C|$ values are statistically higher for peptides with $z = 3$ than $z = 2$. Here, the peak for angiotensin 3+ (A3) has somewhat greater E_C than B2 or other peptides measured, Fig. 5b. The relative position of N2, B2, and A3 features tracks that in macro-FAIMS with t ~100 ms (Fig. 5c), which makes sense for species that are type C already at the smaller $|E_D/N|$. The peaks are broader in Fig. 5b than in Fig. 5c by ~50 times, in line with the prediction upon the acceleration of analysis by ~2700 times (based on R for planar FAIMS scaling[31] as $t^{1/2}$). Had the peak capacity dropped by ~50 times, there would be no noticeable separation in the chip, but the actual difference is ~4 times only. The gain by ~13 times over the $t^{1/2}$ scaling law reflects a similar increase of $|E_C/N|$ values (from 0.12 – 0.18 Td in Fig. 5c to 1.7 – 2.5 Td here) and thus of the separation space width that results from higher $|E_D/N|$ in microchips.

Conclusions

Multichannel FAIMS microchips, which permit maximum electric fields (E_D) >60 kV/cm and filter ions in ~20 μs, were coupled to an ESI source (using a curtain plate/orifice interface with ions injected into the edge of analytical gap) and mass spectrometry. An ion trap MS was used, but any MS platform can be employed. The new ESI/FAIMS/MS system was evaluated for analyses of small ions, amino acids, and peptides, including realistic samples with extensive chemical noise.

Tuning of gas flows in the front and rear FAIMS interfaces permits independent control of the separation time t (that determines the balance between sensitivity and resolving power R) and ion desolvation prior to FAIMS. The measured dependences of R on t and of the separation parameters on E_D match the established scaling laws and *a priori* simulations of ion dynamics including anisotropic diffusion, showing that known FAIMS theory applies at extreme fields. Despite a lower resolving power compared to FAIMS devices with macroscopic gaps, the present chips are able to filter an amino acid from a complex matrix. Perhaps of more utility is the collective separation of peptide ions from common contaminants in the same m/z range (e.g., PEGs). Resolving different peptides is challenging, but may be possible even for those of same charge state. The separation power of macro-FAIMS is often improved by the optimization of gas composition,[16,37,45] including the use of mixtures such as He/N_2, and/or heating the gas,[14] which reduces its number density N and thus increases E/N in proportion to the temperature T. The benefits of these approaches for FAIMS chips are being explored. Still, the resolving power of FAIMS chips would likely remain below the maximum provided by units with macroscopic gaps and extended separation time,[16] rendering these chips most useful for rapid selection of compound classes rather than differentiation of specific ions.

A lower instrumental resolving power does not necessarily translate into lower resolution in practical analyses constrained by separation time. For example, the peak capacity of macro-FAIMS for tryptic peptides is ~15, yet the actual separations used only 3 – 5 steps because the E_C spectrum had to be obtained during the elution of single LC peak.[23,24] Thus the effective peak capacity was just 3 – 5, which is close to that of the present chip.

At higher E_D, the ion-molecule collisions gain energy and thus increasingly involve bouncing off the repulsive wall of the potential surface rather than sampling its well. This change converts many light ions that in previous FAIMS analyses behaved as type A (for which mobility increases in stronger fields) to type C (mobility decreases in stronger fields).

NIH-PA Author Manuscript

NIH-PA Author Manuscript

NIH-PA Author Manuscript

The ultrafast FAIMS/MS capability is expected to open new applications and facilitate high-throughput analyses. From the fundamental perspective, the present development allows the FAIMS characterization of transport properties and ion-molecule potentials for mass-selected ions to be extended to a hitherto inaccessible region.

Acknowledgments

Portions of this work were supported by the Battelle Independent R&D program and the NIH National Center for Research Resources. We thank Dr. Erin S. Baker for her samples and mobility measurements of peptides.

References

1. McDaniel, EW.; Mason, EA. Transport Properties of Ions in Gases. Wiley, NY: 1988.
2. Eiceman, GA.; Karpas, Z. Ion Mobility Spectrometry. Boca Raton, FL: CRC Press; 2004.
3. Shvartsburg, AA. Differential Ion Mobility Spectrometry: Nonlinear Ion Transport and Fundamentals of FAIMS. Boca Raton, FL: CRC Press; 2008.
4. Mukhopadhyay R. Anal. Chem 2008;80:7918–7920. [PubMed: 18975862]
5. Guevremont R. J. Chromatogr. A 2004;1058:3–19. [PubMed: 15595648]
6. Becker C, Qian KN, Russell DH. Anal. Chem 2008;80:8592–8597. [PubMed: 18937419]
7. Tang K, Li F, Shvartsburg AA, Strittmatter EF, Smith RD. Anal. Chem 2005;77:6381–6388. [PubMed: 16194103]
8. Belov ME, Clowers BH, Prior DC, Danielson WF, Liyu AV, Petritis BO, Smith RD. Anal. Chem 2008;80:5873–5883. [PubMed: 18582088]
9. Bohrer BC, Merenbloom SI, Koeniger SL, Hilderbrand AE, Clemmer DE. Annu. Rev. Anal. Chem 2008;1:293–327.
10. Kolakowski BM, Mester Z. Analyst 2007;132:842–864. [PubMed: 17710259]
11. Xia YQ, Wu ST, Jemal M. Anal. Chem 2008;80:7137–7143. [PubMed: 18652493]
12. Pringle SD, Giles K, Wildgoose JL, Williams JP, Slade SE, Thalassinos K, Bateman RH, Bowers MT, Scrivens JH. Int. J. Mass Spectrom 2007;261:1–12.
13. Ruotolo BT, Benesch JLP, Sandercock AM, Hyung SJ, Robinson CV. Nat. Protoc 2008;3:1139–1152. [PubMed: 18600219]
14. Barnett DA, Belford M, Dunyach JJ, Purves RW. J. Am. Soc. Mass Spectrom 2007;18:1653–1663. [PubMed: 17662612]
15. Shvartsburg AA, Tang K, Smith RD. J. Am. Soc. Mass Spectrom 2004;15:1487–1498. [PubMed: 15465362]
16. Shvartsburg AA, Li F, Tang K, Smith RD. Anal. Chem 2006;78:3706–3714. [PubMed: 16737227]
17. Miller RA, Nazarov EG, Eiceman GA, King AT. Sens. Actuat. A 2001;91:301–312.
18. Eiceman GA, Krylov EV, Tadjikov B, Ewing RG, Nazarov EG, Miller RA. Analyst 2004;129:297–304. [PubMed: 15042159]
19. Schmidt H, Tadjimukhamedov F, Mohrenz IV, Smith GB, Eiceman GA. Anal. Chem 2004;76:5208–5217. [PubMed: 15373463]
20. Kendler S, Lambertus GR, Dunietz BD, Coy SL, Nazarov EG, Miller RA, Sacks RD. Int. J. Mass Spectrom 2007;263:137–147.
21. Tang, K.; Shvartsburg, AA.; Smith, RD. US Patent. 7,339,166. 2008.
22. Mabrouki R, Kelly RT, Prior DC, Shvartsburg AA, Tang K, Smith RD. J. Am. Soc. Mass Spectrom. (in press), doi: 10.1016/j.jasms.2009.05.019.
23. Venne K, Bonneil E, Eng K, Thibault P. Anal. Chem 2005;77:2176–2186. [PubMed: 15801752]
24. Canterbury JD, Yi XH, Hoopmann MR, MacCoss MJ. Anal. Chem 2008;80:6888–6897. [PubMed: 18693747]
25. Shvartsburg AA, Li F, Tang K, Smith RD. Anal. Chem 2007;79:1523–1528. [PubMed: 17297950]
26. Robinson EW, Shvartsburg AA, Tang K, Smith RD. Anal. Chem 2008;80:7508–7515. [PubMed: 18729473]

NIH-PA Author Manuscript

NIH-PA Author Manuscript

NIH-PA Author Manuscript

27. Shvartsburg AA, Smith RD, Wilks A, Koehl A, Ruiz-Alonso D, Boyle B. Anal. Chem 2009;81:6489–6495. [PubMed: 19583243]
28. Meek, JM.; Craggs, JD. Electrical Breakdown of Gases. Wiley, NY: 1978.
29. Purves RW, Guevremont R. Anal. Chem 1999;71:2346–2357.
30. Shvartsburg AA, Tang K, Smith RD. J. Am. Soc. Mass Spectrom 2005;16:1447–1455. [PubMed: 16006140]
31. Shvartsburg AA, Smith RD. J. Am. Soc. Mass Spectrom 2007;18:1672–1681. [PubMed: 17723907]
32. Krylov EV, Nazarov EG, Miller RA. Int. J. Mass Spectrom 2007;266:76–85.
33. Javahery G, Thomson BA. J. Am. Soc. Mass Spectrom 1997;8:697–702.
34. Barnett DA, Ells B, Guevremont R, Purves RW. J. Am. Soc. Mass Spectrom 1999;12:1279–1284.
35. Guevremont R, Barnett DA, Purves RW, Viehland LA. J. Chem. Phys 2001;114:10270–10277.
36. Barnett DA, Ells B, Guevremont R, Purves RW, Viehland LA. J. Am. Soc. Mass Spectrom 2000;11:1125–1133. [PubMed: 11118120]
37. Barnett DA, Ells B, Guevremont R, Purves RW. J. Am. Soc. Mass Spectrom 2002;13:1282–1291. [PubMed: 12443018]
38. Guevremont R, Barnett DA, Purves RW, Vandermey J. Anal. Chem 2000;72:4577–4584. [PubMed: 11028613]
39. Barnett DA, Ding L, Ells B, Purves RW, Guevremont R. Rapid Commun. Mass Spectrom 2002;16:676–680. [PubMed: 11921246]
40. Purves RW, Barnett DA, Ells B, Guevremont R. Rapid Commun. Mass Spectrom 2001;15:1453–1456. [PubMed: 11507759]
41. Baker ES, Clowers BH, Li F, Tang K, Tolmachev AV, Prior DC, Belov ME, Smith RD. J. Am. Soc. Mass Spectrom 2007;18:1176–1187. [PubMed: 17512752]
42. Baker ES, Tang K, Danielson WF, Prior DC, Smith RD. J. Am Soc. Mass Spectrom 2008;19:411–419. [PubMed: 18226544]
43. Li J, Taraszka JA, Counterman AE, Clemmer DE. Int. J. Mass. Spectrom 1999;185/186/187:37–47.
44. Shvartsburg AA, Li F, Tang K, Smith RD. Anal. Chem 2006;78:3304–3315. [PubMed: 16689531]
45. Cui M, Ding L, Mester Z. Anal. Chem 2003;75:5847–5853. [PubMed: 14588025]

NIH-PA Author Manuscript

NIH-PA Author Manuscript

NIH-PA Author Manuscript

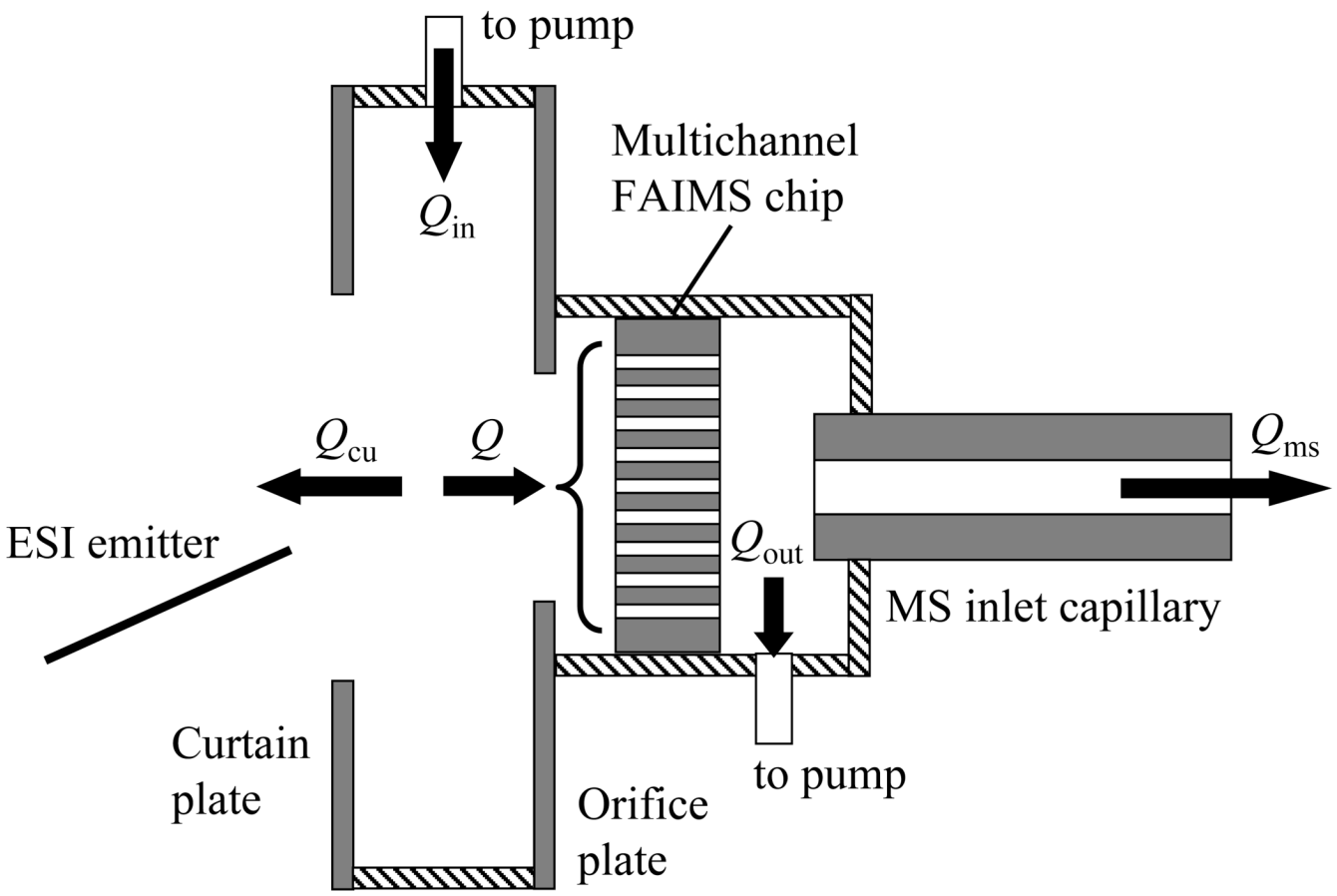

Fig. 1.
Scheme of the ESI/FAIMS/MS interfacing with gas flows (insulating elements are dashed).

NIH-PA Author Manuscript
NIH-PA Author Manuscript
NIH-PA Author Manuscript

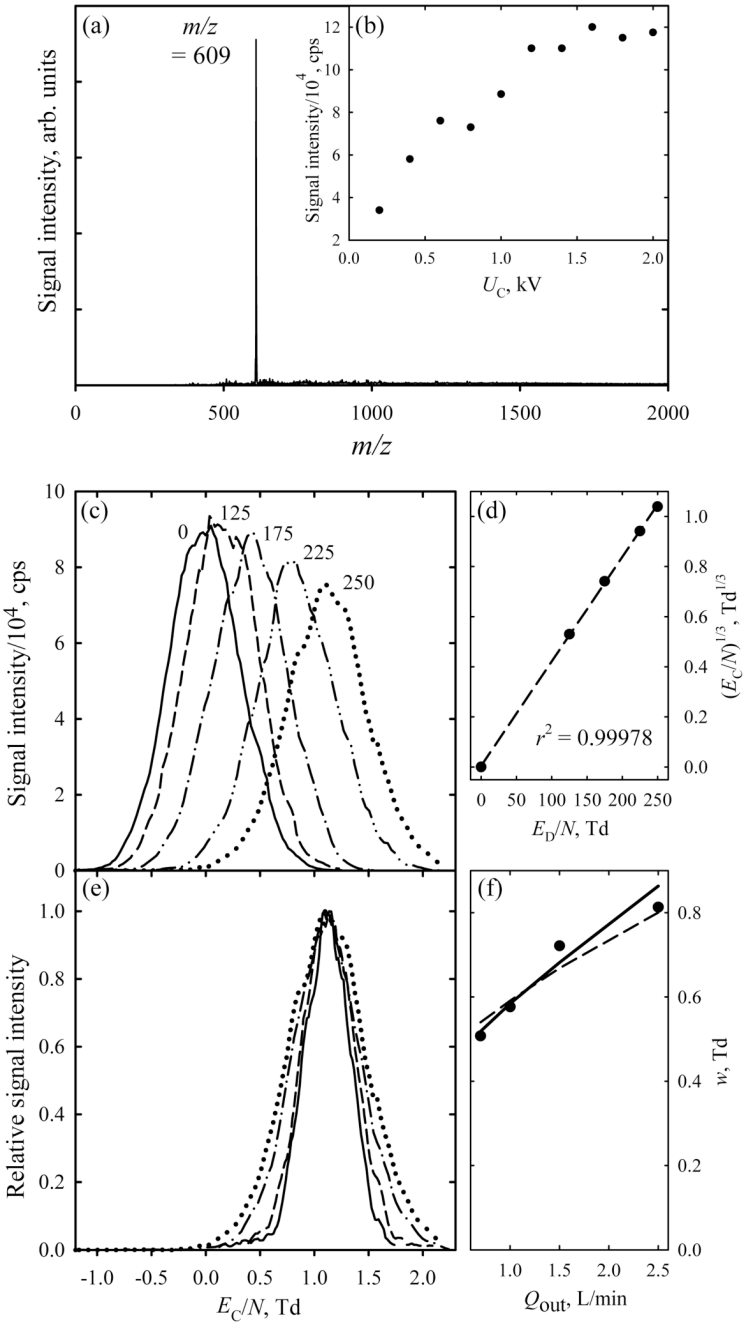

Fig. 2.

FAIMS/MS data for reserpine: (a) total MS spectrum; (b) base peak intensity depending on the curtain plate voltage; (c) FAIMS spectra (Q_{out} = 2.5 L/min) for m/z = 609 at E_D/N values (in Td) as labeled; (d) cubic root of E_C/N values in panel (c) versus E_D/N (circles) and linear regression through the dependence (line); (e) normalized FAIMS spectra for m/z = 609 at E_D/N = 250 Td with Q_{out} of 2.5 (dotted line), 1.5 (dash-dot), 1.0 (dashed), and 0.7 L/min (solid); (f) measured (circles) and calculated (lines) peak widths for the conditions in (e), with solid and dashed lines representing the simulations and the square root scaling with the separation time, respectively.

NIH-PA Author Manuscript
NIH-PA Author Manuscript
NIH-PA Author Manuscript

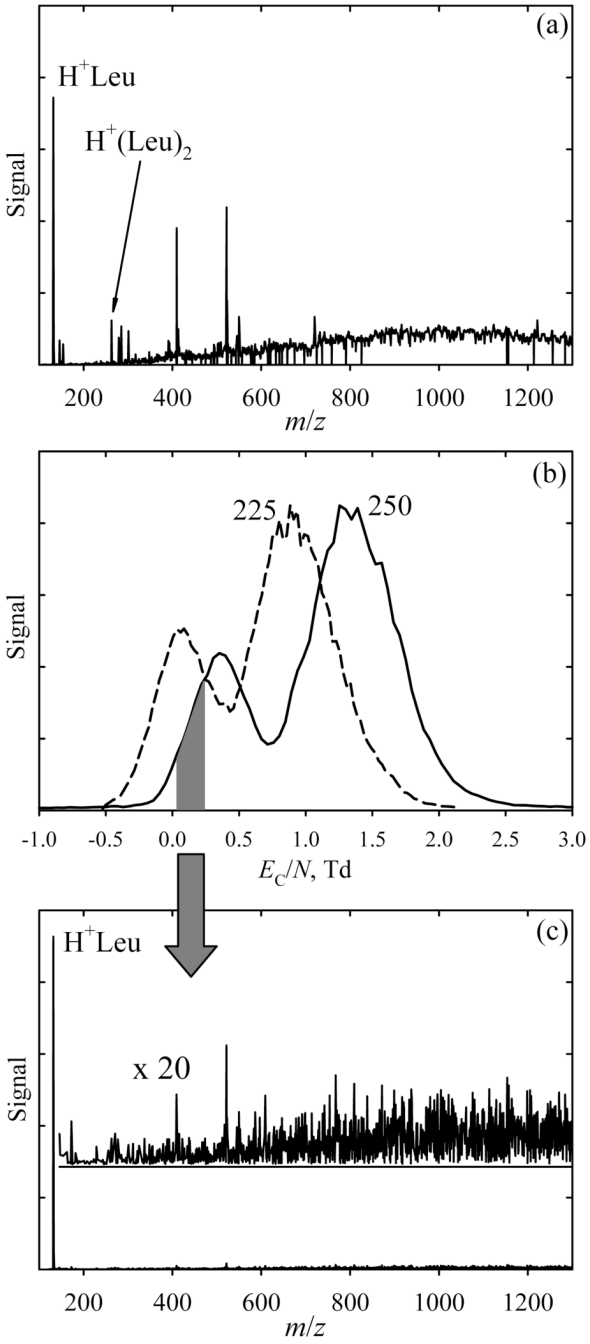

Fig. 3.

Data for leucine solutions in a complex matrix: (a) total MS spectrum; (b) FAIMS spectra for two E_D/N values as labeled (Q_{out} = 1.1 L/min); (c) MS spectrum integrated over the E_C/N range of 0.03 – 0.24 Td marked in (b).

NIH-PA Author Manuscript

NIH-PA Author Manuscript

NIH-PA Author Manuscript

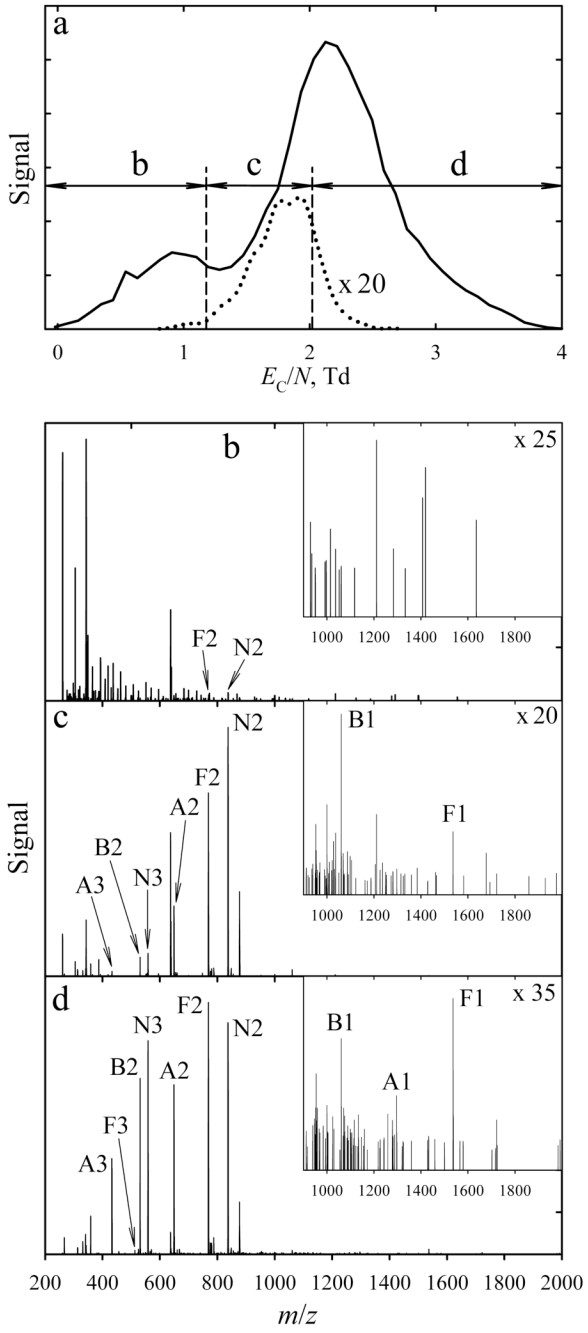

Fig. 4.

Data for peptide solutions in a complex matrix: the FAIMS spectra for all ions (solid line) and bradykinin 1+ (dotted line) measured using Q_{out} = 0.5 L/min at E_D/N = 250 Td (a) and mass spectra over the E_C/N ranges of 0 – 1.2 Td (b), 1.2 – 2.0 Td (c) and 2.0 – 4.0 Td (d) marked in (a), with expansions for high *m*/*z* in the insets. The peak labels have a letter for the peptide ("B" for bradykinin, "A" for angiotensin, "F" for fibrinopeptide, and "N" for neurotensin) followed by a number for the charge state.

NIH-PA Author Manuscript

NIH-PA Author Manuscript

NIH-PA Author Manuscript

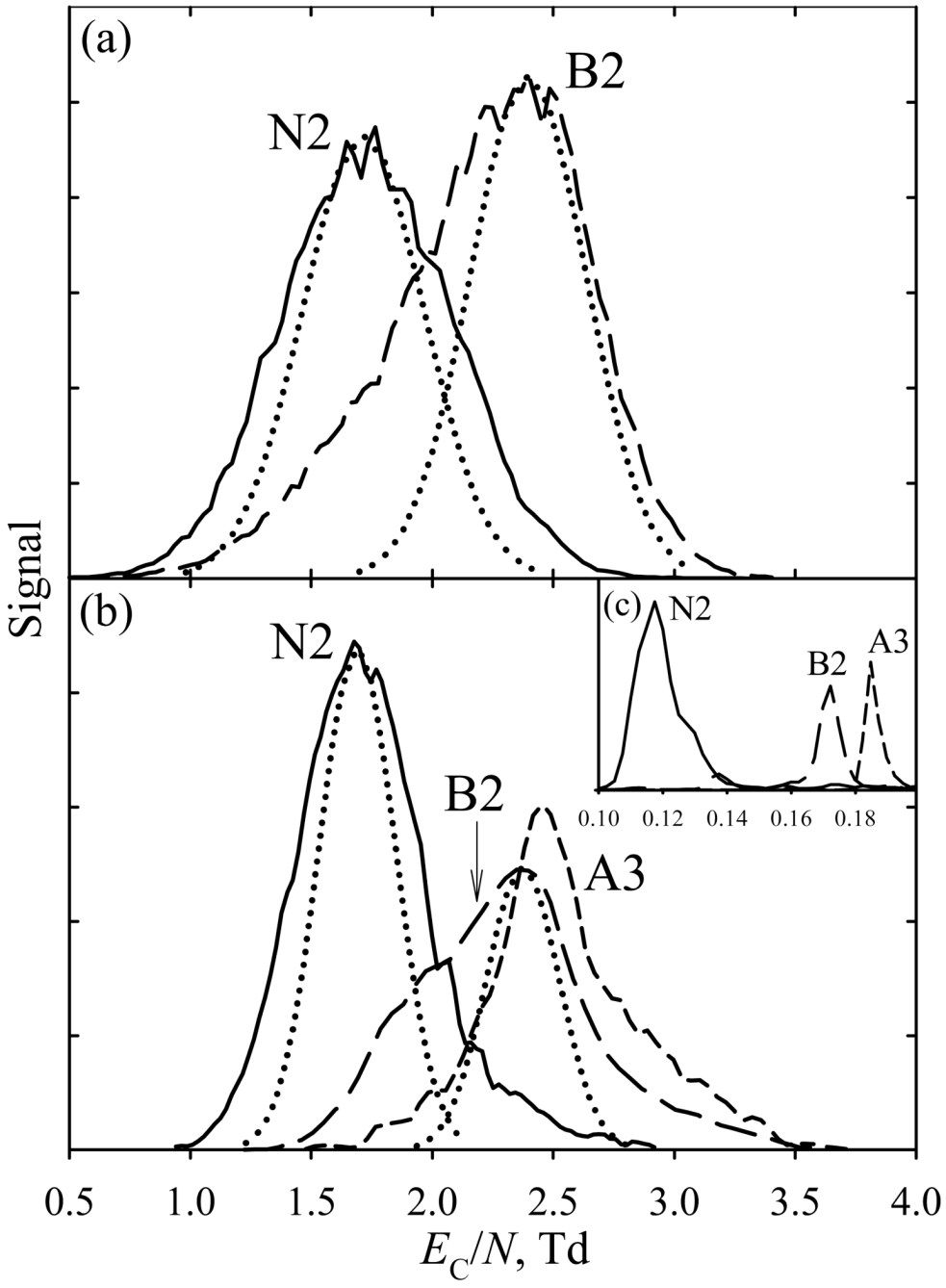

Fig. 5.

Mass-selected FAIMS spectra for exemplary peptides (E_D/N = 250 Td), measurements (solid lines) and modeled peaks (dotted lines) at Q_{out} of 2.5 L/min (a) and 0.5 L/min (b). The spectra for same species (scaled to same peak heights) obtained using planar macro-FAIMS [22] at E_D/N = 86 Td are shown in (c). The nomenclature follows Fig. 4.